Assessing effective connectivity in epileptogenic networks. A model-based simulation approach

Assessing effective connectivity in epileptogenic networks. A model-based simulation approach.

Florencia Jacobacci*[1,2], Martin Sapir*[1,2], Santiago Collavini*[1,2], Silvia Kochen[2], Alejandro Blenkmann[1,2]

1 Facultad de Ingeniería y Ciencias Exactas y Naturales, Universidad Favaloro, Buenos Aires, Argentina
2 IBCN "Prof. E. De Robertis", Facultad de Medicina, Universidad de Buenos Aires (UBA) - CONICET, Buenos Aires, Argentina.

e-mail: florenciajacobacci@gmail.com, martinsapir@gmail.com, santiagocollavini@gmail.com, ablenkmann@gmail.com

Abstract. Different connectivity configurations were simulated using epileptogenic and non epileptogenic neuronal populations. Connectivity between them was measured using Partial Directed Coherence and Directed Transfer Function. The results were satisfactory and in some cases of clinical utility. The methodology that was used is discussed in comparison with previous works.

* Jacobacci, Sapir and Collavini contributed equally to this work.

1. Introduction

Epilepsy is a neurological pathology characterized by the recurrence of seizures which is the result of abnormal electrical activity in groups of neural populations. The *epileptogenic zone* (EZ) is the area of cortex indispensable for the generation of seizures. It may include different overlapped areas: the *seizure onset zone* (SOZ), an abnormal region of the brain which becomes hyperexcitable and synchronized and triggers the epileptic seizure; the *irritative zone* (IZ), an area of cortex involved in epileptic interictal activity; and other areas, e.g. lesion zones [1]. To keep seizures under control, the most common treatment is drug-based. Unfortunately, 30% of these patients do not respond to pharmacological treatment [2] and the surgical treatment, i.e. tissue resection, may be the best option in 50% of these cases [3]. In order to eradicate seizures after cortical resection the EZ has to be correctly defined.

Intracranial electroencephalography (iEEG) recording of brain activity is the gold standard method of assessing the location and extent of the SOZ and IZ since it provides electrical signals directly recorded from the cortical surface (*electrocorticography*, ECoG) or areas deep inside the brain (*StereoElectroencephalograpy*, SEEG). The incorrect identification and resection of the pathological region would result in the recurrence of seizures after surgery. As a consequence, it is crucial to determine its anatomical location, its functional interactions, and its connectivity pattern. The EZ is organized as a network, commonly known as *epileptogenic network*, and is formed by different neuronal populations connected to each other. Understanding this organization may have implications in the surgery prognosis.

It has long been recognized that neuronal interactions are directional [4]. Being able to assess the directionality of neuronal interactions in the EZ is highly desirable in order to have a deeper understanding of the behavior and extension of pathological network.

Different kinds of connections have been defined in neuroscience in the last decades. Anatomical connectivity refers to the physical trajectory of the nervous fibers that connect different regions of the brain. This type of connectivity is almost stable over time and can be assessed using diffusion tensor imaging. Functional connectivity is a concept that reflects the functional interaction of different temporal correlations between remote neurophysiological events. It is simply a statement about the observed correlations; it does not provide any direct insight into how these correlations are mediated. Functional connectivity is studied using functional neuroimaging techniques such as functional magnetic resonance imaging (fMRI). Effective connectivity, on the other hand, is closer to the intuitive notion of a connection and can be defined as the influence on neural system exerts over another. This connectivity may vary over different situations, conditions or tasks, denoting the dynamics of information processing between different areas in the brain. In pathological situations, as in epilepsy, evidence indicates that effective connectivity may be affected [5][6]. A significantly different connectivity pattern distinguishes the epileptogenic zone from other cortical regions not only during the ictal event, but also during the inter- and pre-ictal periods. This indicates that the lesional nodes play a leading role in generating and propagating ictal EEG activity by acting as the hubs of the epileptic network originating and sustaining seizures.

The aim of this work is to be able to test tools that estimate the effective connectivity between neuronal populations within the epileptogenic network. The knowledge of this characteristic would offer better insight on the pathology and a better planning of resection surgery, resulting in a better quality of life for the patient. In order to study the reliability of the connectivity estimator, we propose the use of non-linear physiologically plausible models of neuronal populations. These models have proven to be useful in resembling real iEEG signals [7]. Besides, they allow variation of the parameters so as to set the connectivity between the different groups of neurons.

2. Method

To test the reliability of the connectivity estimators, we generated a series of data representing pairs of populations with different characteristics and different connectivity. These populations consisted of epileptic and/or non-epileptic neurons with a one-way connectivity gain. We defined three different levels of coupling based on the activity induced by an epileptogenic population over a non-epileptogenic one. These levels were denoted as low, intermediate and high. Four basic cases were defined in which all the possible combinations of said populations were represented. Each case was simulated four times, according to high, medium and low connectivity or none at all, thus defining sixteen different series of data.

Lastly, two final simulations were carried out with three populations which represented a more relevant and realistic case. The connectivity was measured using Partial Directed Coherence and Directed Transfer Function [8][9][10]. Statistical significance of connectivity measurements was tested using a non-parametric surrogate statistical method. Phase randomized surrogate data was used for the tests [11]. Finally, to account for multiple comparisons statistics, the false discovery rate (FDR) method was applied [12].

All simulations and data analysis were done in Matlab 7.12.0 (The MathWorks, Inc). Our own scripts were developed and functions from ARFIT, BIOSIG, EEGLAB and SIFT toolboxes for Matlab were also used for this purpose [13][14][15][16][17].

2.1. Physiologically plausible model

The model used is a reversion of a neurophysiologically relevant model which represented the generation of evoked potentials in the visual cortex [18]. Later on, this model was extended to generate spontaneous interictal spikes from multiple coupled neuronal populations by altering the

model parameters [7]. The simulation of this kind of pathological electrical activity has successfully been used to evaluate sLORETA algorithm for the resolution of the inverse problem on ECoG [19].

The diagram of the model used to simulate normal and epileptic brain activity in a realistic way can be seen on Figure 1. On this model, each population represents thousands of neurons and is composed of three subpopulations: pyramidal neurons, excitatory inter-neurons, and inhibitory inter-neurons. In turn, each subpopulation is characterized by: a) a non-linear sigmoid function S(v) that relates the average membrane potential of the subpopulation with the density of action potentials and b) a second order linear system which relates the density of pre-synaptic impulses to the average membrane potential; excitatory post-synaptic potential (EPSP) or inhibitory post-synaptic potential (IPSP), depending if the generating subpopulation is excitatory or inhibitory. Besides, there are four constants C_i (i=1, 2, 3, 4) that represent the amount of synapses between the subpopulations.
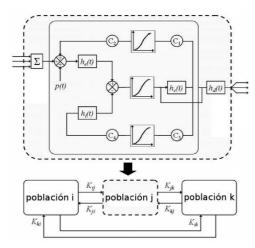

Figure 1. Physiologically plausible model of coupled neural populations. The top of the figure shows the diagram for a cortical population where the upper loop represents the subpopulation of excitatory inter-neurons, the middle loop represents pyramidal neurons and the lower loop represents inhibitory neurons. On the bottom of the figure, connection with other populations can be seen.

The impulse response of the second order systems represents the EPSP and IPSP of the modeled neurons. In the case of pyramidal neurons and excitatory inter-neurons this is $h_e(t)=Aate^{-at}$ whereas for inhibitory inter-neurons it is $h_i(t)=Bbte^{-bt}$, where A and B are the average synaptic gains for each model, and a and b are linked to the membrane average time constant and the average distributed delays in the dendritic tree. In normal conditions, A=3,25mV, B=22mV, a=100s−1 and b=50s−1. The populations modeled using these parameters are called *passive* and the electrical activity they generate is "background activity". On the other hand, increasing the average excitatory synaptic gain to values between 3,4mV and 3,6mV leads these populations to a state of rhythmic generation of interictal spikes. These populations are called *active*.

Finally, to define the coupling between the populations, the matrix K is used, where each element K_{ij} represents the coupling intensity between the origin population *i* with the destiny population *j*.

The mean membrane potentials in pyramidal neurons are a measure of the neural activity in a relatively small area of cortex and are proportional to the potentials recorded with intracranial electrodes [19]. Therefore, these signals are used as output of the system. The coupling parameters define the connectivity between populations and can be adjusted to simulate different network configurations.

A coupling criterion was defined based on the behavior of a *passive* neuron when receiving information from an *active* one. The passive neuron would start to show spikes with a firing rate related to the coupling parameter. At a certain level of coupling the passive neuron would have a firing rate equivalent to that of the active neuron (at least 30 spikes per minute); this level was defined as high connectivity. Low connectivity was defined as the lowest level that produces a firing rate different than zero (about 5 spikes per minute). A third, intermediate level was defined in between these two.

The assessed connectivity estimators presented later in this work may predict these configurations based on the information of membrane potential in the pyramidal neuron populations. These potentials

were selected as an appropriate measure since real iEEG recordings are proportional to the mean membrane potential of pyramidal neurons populations. The reader is referred to [7] and [18] for more details of the model used.

2.2. Multivariate causality based measures of connectivity

The methods for studying effective connectivity between neuronal populations were based on mathematical analysis of the membrane potential in the pyramidal neuron populations. These data were presented in the form of multiple simultaneous time series.

The basic concept of bivariate causality introduced by Granger is the causal influence in the context of linear regression models. If the variance of the autoregressive prediction error of one time series at the present time is reduced by inclusion of past measurements from a second time series, then the second is said to have causal influence on the first i.e. the prediction of one time series could be improved by incorporating the knowledge of a second one [4][20].

2.2.1. Multivariate autoregressive (MVAR) model Let $X(t)=[X_1(t),\ X_2(t),...,X_k(t)]^T$ denote the measurement from k channels at time t and *T means* matrix transposition. We can describe $X(t)$ in the form of a MVAR model [9]. In equation 1, p is the model order, that is to say, how many previous values of X are needed to estimate the current value. $A(i)$ is a matrix of dimension kxk containing the autoregressive coefficients A_{mn}, m and $n=1,...,k$ which relate channel m with channel n for the time lag i. $E(t)$ is a vector of length k containing the error term for each channel, i.e. part of the signal X at time t that is not explained by the previous values of X.

$$X(t) = \sum_{i=1}^{p} A(i)X(t-i) + E(t) \tag{1}$$

2.2.2. Directed Transfer Function In the definition of Granger causality given at the beginning of section 2.2, only two time series are considered. Directed Transfer Function (DTF) is a multivariate method that gives pairwise directional information from one autoregressive model fit to a larger number of channels. It has been shown that multivariate DTF function can be interpreted within the framework of Granger causality [9] . Transforming equation 1 to the frequency domain [8], we obtain:

$$A(f) = I - \sum_{j=1}^{p} A(j)exp(-i2\pi f \Delta tj) \tag{2}$$

Where I is the identity matrix of dimension k x k and Δt is the sampling interval.

Equation 2 can be rewritten as:

$$X(f) = A^{-1}(f)E(f) = H(f)E(f) \tag{3}$$

In equation 3, $H(f)$ is the transfer matrix of the system for each time frequency point.

DTF from channel j to channel i, representing the causal influence from j to i at frequency f, is defined as:

$$\theta_{ij}^2(f) = \left|H_{ij}(f)\right|^2 \tag{4}$$

The normalized DTF expresses the ratio of influence of channel j to channel i to the joint influences from all the other channels to the channel i, and has a value between 0 and 1.

$$\gamma_{ij}^2(f) = \frac{\left|H_{ij}(f)\right|^2}{\sum \left|H_{im}(f)\right|^2} \tag{5}$$

It is important to highlight that a zero value of DTF may not mean a total absence of causal influence between the two channels [9].

2.2.3. Partial Directed Coherence Partial Directed Coherence (PDC) was introduced as a modification/generalization of directed coherence and DTF. While DTF represents a balance of signal

power that spreads from one structure to another over many possible alternative pathways, PDC portrays the relative strength of direct pairwise interactions. As a consequence, DTF marks the existence of signal pathways connecting structures either directly or indirectly while PDC resolves the existence of direct connections[23]. Thus, PDC provides clearer and more immediate frequency domain connectivity picture of Granger causality for the simultaneous analysis of more than two time series [10]. Besides, PDC has the computational advantage of avoiding the matrix inversion in equation 3 that the calculation of DTF requires.

The normalized squared PDC expresses the ratio of influence of channel j to channel i to the joint influences from channel j into all other channels, and has a value between 0 and 1.

$$\pi_{ij}^2(f) = \frac{\left|A_{ij}(f)\right|^2}{\sum \left|A_{im}(f)\right|^2} \qquad (6)$$

2.3. Simulation of data, adjustment of MVAR model and calculation of DTF and PDC

Sixty seconds simulations were considered a good balance between the number of data points to synthesize and analyze and sufficient interictal record with abundant epileptic spikes. Based on previous studies sampling frequency was set to 200 Hz [23]. Average excitatory synaptic gain was set to 3.25mV to generate passive populations and to 3.52mV to generate active ones. Null, low, medium and high one-way connectivity between the populations were used.

Two coupled poupulations

Four groups were defined according to the populations and direction of connectivity possibly involved in a simulation consisting of two populations. The name of each group consists of two characters that identify the type of neurons that take part of the coupling as passive (P) or active (A). The first character refers to the population where the information flow is originated and the second one refers to the population which is the destiny of this flow.

These groups were simulated for each connectivity level: null (N), low (L), intermediate (M) and high (H). Simulations will be quoted using this code (e.g.: simulation PA-M refers to a passive population coupled to an active one with intermediate connectivity with the information flowing from the passive to the active population). The result was 15 simulations (due to AP-N and PA-N being equivalent) which cover all the possible combinations of unidirectional and null connectivity between active and/or passive populations.

Many coupled populations

The two final cases represented an active population (A) connected to a passive one (P1), which in turn was connected to another passive population (P2). The coupling scheme used can be seen in figure 2. Connectivity between the active population A and the passive population P1 (A→P1) was set to be medium. Two different connectivity patterns were assumed. In one of these cases the connectivity between the passive populations (P1→P2) was set to be low (this case will be quoted as APP-ML), while in the other it was set to be medium (which will be quoted further in this work as APP-MM).
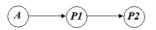

Figure 2. Coupling scheme for APP-ML and APP-MM simulations.

Since spike duration is 200-300 ms long, and based on physiological previous works [6] we constrained the MVAR model to use information from the previous 100ms to estimate the actual signal value. Therefore, the time series data were adjusted using an order 20 MVAR. To test this premise, the Schartz Bayes Criterion (SBC) was used to define an optimal MVAR model order. The Matlab ARFIT Toolbox was used for this purpose [13][14].

The connectivity is most likely to be time variant in this case due to the mutual influence of brain regions [21]. As a consequence, a Kalman filter was used to estimate the MVAR model coefficients on

every time sample using Matlab's Biosig toolbox [15]. Then, PDC and DTF were calculated for every time point and every frequency going from 0 to Nyquist frequency using our own Matlab scripts. PDC and DTF were chosen over the multivariate version of Granger causality [22] due to the fact that PDC and DTF consider the frequency domain and they are normalized estimators of connectivity [23].

2.4. Non-parametric statistical test for significance

An empirical distribution technique using surrogate data was used [9],[11]. Surrogate data were constructed by performing an independent phase randomization in each of the time series data. This method has no assumptions about connectivity distributions and allows testing a no connection hypothesis. The data was transformed using Matlab fast Fourier transform command. The phase was then randomized independently for each channel, making sure that the phase spectrum remained odd. Afterwards, the signal is transformed to the time domain using inverse fast Fourier transform. Phase randomization algorithm maintains the power spectrum of the signal while destroying any information flow in the time domain.

In order to have good statistical significance, we created an empirical distribution for the causal measures out of 500 surrogates. Since phase randomization method assures that there is no interaction among the channels, this distribution gives the estimator behavior for the null hypothesis case. P-value of every time-frequency was obtained in comparison with the surrogate distribution.

2.5. Multiple comparison statistics

The approach on assessing statistical significance of the results that was discussed in the previous section bears a probability that there will be false positive detections. Considering the fact that the connectivity matrix has a time-frequency dimension of 600000 points (50 frequency by 12000 time points), approximately 3000 points may show a statistically significant connectivity due to the multiple comparisons (assuming that the null hypothesis is true, alpha value of 0.05 and a normal distribution of the connectivity estimator). In order to correct for multiple comparisons a false discovery rate (FDR) method was applied to the connectivity matrix which eliminated false results with a 5% error rate. The implementation for the FDR method belongs to the SIFT toolbox for EEGlab [16][17].

3. Results

The simulated model of the neural populations proved to be effective, as it resulted in a physiologically plausible signal in which the algorithms could be tested. Active and passive populations were simulated in different cases so as to represent the different combinations of populations that could be present in the neural cortex.

To fulfill the criteria described in section 2, connectivity coupling parameters K were defined as 100, 170 and 275 for low, medium and high simulations respectively.

The order 20 MVAR showed little to no difference compared to lower orders despite the fact that the SBC is known to penalize for the use of a large order model. As a matter of fact, it is more acceptable to err due to overfitting rather than subfitting, hence the preference over the largest order. On figure 3, SBC for simulation AP-L can be seen. Similar results were obtained for the rest of the simulations. According to SBC, MVAR model order should be between 3 and 25 depending on the considered simulation.
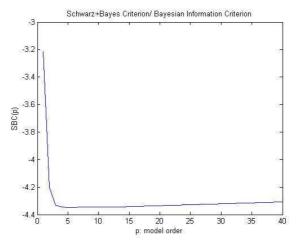
Figure 3. Bayesian criterion shows that the chosen model order is
acceptable

Connectivity was measured in these simulations, and the effectiveness of the PDC and DTF algorithms turned out to be determined by the neuronal populations involved. Since the simulations involving two coupled populations can not include indirect connectivity between them, results of PDC and DTF did not differ in those cases. As expected, in the many coupled populations, some differences were found in the estimation of connectivity using PDC and DTF [10],[23].

Non-coupled populations

Simulations PP-N, AA-N and PA-N (equivalent to AP-N) were estimated correctly, as the PDC and DTF plots ended up being void of all information.

Groups PA, PP and AA

In most cases, the effective connectivity measurements properly showed the coupling direction among populations until the surrogate data method and the statistical test for significance were applied, resulting in the equivalent of no connectivity at all between the populations. This would suggest that the method has low sensitivity for this kind of application.

Group AP

Connectivity measures from simulations AP-H and AP-M are showed in figures 4 and 5 respectively. Different frequency connectivity patterns can be observed. Connectivity results in simulation AP-L were not statistically significant when contrasted with the no connectivity hypothesis.
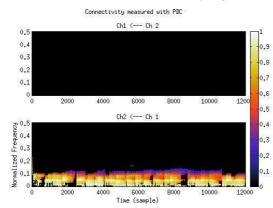

Figure 4. PDC of simulation AP-H. The connectivity is mainly in the lower frequency band. Ch1: A population, Ch2: P population.
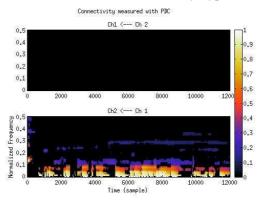
Figure 5. PDC of simulation AP-M. The connectivity is mainly in the lower frequencies and also spread over medium frequencies. Ch1: A population, Ch2: P population.

Many coupled populations

PDC and DTF results for simulation APP-MM can be seen on figures 6 and 7, respectively. Differences between PDC and DTF were visible in these cases. Significant connectivity was measured for A→P1 and P1→P2. DTF in this case did not depict the indirect connectivity between A and P2, as it could be expected [9].

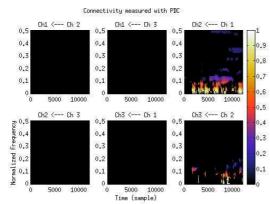**Figure 6.** PDC for APP-MM simulation. A→P1 and P1→P2 show effective connectivity in the lower frequency band. P1→P2 connectivity shows lower strength. Ch 1: A population, Ch 2: P1 population, Ch 3: P2 population.

Figure 7. DTF for APP-MM simulation. A→P1 and P1→P2 show effective connectivity in the lower frequency band. P1→P2 connectivity shows lower strength. Ch 1: A population, Ch 2: P1 population, Ch 3: P2 population.
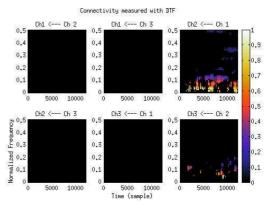
PDC and DTF results for simulation APP-ML can be seen on figures 8 and 9, respectively. Connectivity was measured successfully for A→P1 but a non significant measure was found for P1→P2. Again, the difference between DTF and PDC measures can be seen. DTF for APP-ML depicts a very low indirect connection between A and P2.
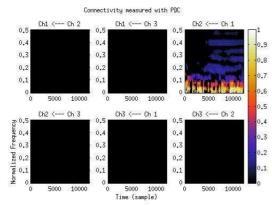

Figure 8. PDC for APP-ML simulation. A→P1 show effective connectivity mainly in the lower frequency band. P1→P2 connectivity is not detected. Ch 1: A population, Ch 2: P1 population, Ch 3: P2 population.
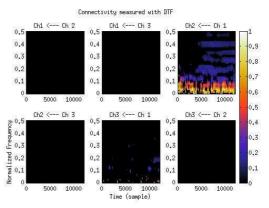
Figure 9. DTF for APP-ML simulation. A→P1 show effective connectivity mainly in the lower frequency band. P1→P2 connectivity not detected. Indirect connectivity is measured between A→P2 Ch 1: A population, Ch 2: P1 population, Ch 3: P2 population.

4. Discussion and conclusion

Results show that PDC and DTF methods, corrected by FDR method, describe correctly the connectivity for simulations AP-M, AP-H, PP-N, AA-N and PA-N (equivalent to AP-N). On

simulation AP-L, the measured connectivity was not significant. This could be due to the fact that low connectivity gain was defined as the least possible to alter the firing rate of the passive population, thus providing little information flow. As a consequence, causal influence resolution achieved by the method may be below what we expected to resolve.

The estimation of connectivity in the simulations belonging to group PA and PP was not significant. This might be caused by the fact that information coming from passive populations does not modify the firing rate of the destiny populations. As for simulations of group AA, results were not significant either. This could be due to the non-linearity of the signals, which would make it difficult for the MVAR model to get a good estimation of the temporal dynamics of this signal.

The fact that the best outcome came from simulations AP-M and AP-H shows that the estimation of connectivity between two populations using this method might be only possible when the firing rate of the destiny population is noticeably altered.

Three population simulations offer a more realistic approach of the connectivity on an epileptogenic network. Connectivity from the active population A to the passive P1 was measured for simulations APP-MM and APP-ML with both PDC and DTF. These results are of importance in the clinical interpretation of epilepsy network configuration, since this method allows the determination of how epileptic activity is spread from its origin. Meanwhile, connectivity from P1 to P2 could only be measured in simulation APP-MM. These simulations use the passive population in the middle of the connectivity path as an information pathway. Again, the case is properly represented by PDC and DTF once the firing rate in the destiny populations is altered in a noticeable way. Since P1 is a passive population "activated" by A, the coupling P1→P2 behaves more like an AP coupling than a PP coupling. PDC and DTF for AP-L simulation proved to be not significant while AP-M did. As a consequence, the results for many coupled populations are consistent with what was found for simulations of two coupled populations.

We noticed differences in the frequency response of PDC and DTF according to the strength of couplings. These differences will be studied in future works.

As PDC and DTF methods are linear estimators it is evident that the connectivity estimation will be more effective in signals simulated by the use of linear models. Previous works have already proven the success of DTF and PDC for estimation of signals generated linearly via autoregressive simulation [23]. Recent work has been done on estimating connectivity based on simulated data of physiological significance [28]. However this work is based on a two-dipole model with linear dynamics which is far from representing the non-linear dynamics of real brain signals.

Astolfi et al. [26] simulated a non-linear population model signal [7] and then other population signals to simulate a neural network. However, the other populations with connections to the non-linear one were generated based on delays and escalations of it [26]. This type of connections were well described by PDC, however physiological plausibility of this signals is not clear.

It is important to remark that, in this work, we applied the model proposed by Wendling et al. [7] which is representative of the physiological reality. This means PDC and DTF's effectiveness was tested with a model that generates physiologically plausible neuronal signals. However, PDC and DTF are linear estimators of causal influence. Using non-linear connectivity estimators may provide better results, since this model includes non-linear elements and it has been shown that subtle relations between signals are not accessible by linear methods [27].

In [7] the authors proposed the use of a nonlinear method to analyze the connectivity of simulated signals, the nonlinear correlation coefficient h2 to measure the degree of coupling between two signals. Although h2 proved to be effective at estimating the connectivity between two nonlinear signals, it does not give information about the flow direction of the information.

DTF has already been used to study the propagation of epilepsy real neural information using intracranial recordings [8]. However, it is to be noted that no statistical tests for significance were applied. In our work we have observed that the use of FDR reduces considerably the number of connections that are noticed.

It should also be noted we did not attempt any pre processing of the data, which may help improve the statistical significance in the results. Also, the use of other methods for multiple comparisons corrections, such as voxel-cluster approach, may provide more consistent results [1]

For future works, attempting to pre-process the data may produce more sensible results. Some possibilities include a normalization based on the variance of the signals. It remains unclear, yet, how to consider the influence of interictal spikes in this procedure. Moreover, an approach analyzing only interictal spikes is interesting. Besides, the use of information theory approach will avoid the linearity constrains that are used in PDC and DTF.

Concluding, we evaluated the use of PDC and DTF as estimators of effective connectivity between philologically plausible populations in epilepsy. The methods show sensitivity to distinguish the coupling from active to passive populations at intermediate and high levels. This tool may be useful in the description of epileptogenic networks. However other techniques would be necessary to achieve more sensible results.

References

[1] Rosenow F and Lüders H S 2001 *Brain* **124** 1683-700
[2] Kwan P et al. 2010 Definition *Epilepsia* **51** 1069-77
[3] Engel J 1998 *Epilepsy Res.* **32** 1-11
[4] Ding M, Chen Y and Bressler S L 2006 in Handbook of Time Series Analysis
[5] Van Mierlo P et al. 2013 *Epilepsia,* In press
[6] Varotto G, Tassi L, Franceschetti S, Spreafico R, Panzicca F 2012 *NeuroImage* **61** 591-8
[7] Wendling F, Bellanger J J, Bartolomei F and Chauvel P 2000 *Biol. Cybern.* **83** 367–78
[8] Ge M, Jiang X, Bai Q, Yang S, Gusphyl J and Yan W 2007 *Conference proceedings: Annual International Conference of the IEEE Engineering in Medicine and Biology Society*
[9] Kaminski M, Ding M, Truccolo W A and Bressler S L 2001 *Biol. Cybern.* **85** 145–57
[10] Sameshima K and Baccalá L A 1999 *Journal of neuroscience methods* **94** 93–103
[11] Theiler J, Eubank S, Longtin A, Galdrikian B, and Doyne Farmer J 1992 *Physica D* **58** 77–94
[12] Genovese C R, Lazar N A and Nichols T 2002 *NeuroImage* **15** 870–8
[13] Neumaier A and Schneider T 2001 *ACM Trans. Math. Softw.* **27** 27-57
[14] Schneider T and Neumaier A 2001 *ACM Trans. Math. Softw.* **27** 58-65
[15] Available at: http://biosig.sourceforge.net/
[16] Mullen T, Delorme A, Kothe C and Makeig S 2010 An Electrophysiological Information Flow Toolbox for EEGLAB Society for Neuroscience Conference, San Diego, CA, USA, 2010
[17] Delorme A, Mullen T, Kothe C et al 2011 EEGLAB, SIFT, NFT, BCILAB, and ERICA: New Tools for Advanced EEG Processing *Computational Intelligence and Neuroscience* **2011**
[18] Jansen B H and Rit V G 1995 *Biol. Cybern.* **366** 357–66
[19] Blenkmann A, Beltrachini L, von Ellenrieder N, Kochen S, Muravchik C H 2011 *XIV Reunión de trabajo en Procesamiento de la Información y Control*
[20] Granger C W J 1969 *Econometrica* **37** 424-38
[21] Omidvarnia A, Mesbah M, O'Toole J M, Colditz P, Boashash B 2011 *7th International Workshop on Systems, Signal Processing and their Applications (WOSSPA)*
[22] Barrett A B, Barnett L, Seth A K 2010 *Physical Review E* **81** 041907
[23] Baccalá L A and Sameshima K 2001 *Biol. Cybern.* **84** 463-74
[24] Blenkmann A 2012. PhD Thesis UNLP. Available at: http://sedici.unlp.edu.ar
[25] Haufe S, Nikulin V V, Müller K R and Nolte G 2013 *NeuroImage* **64** 120-33
[26] Astolfi L et al. 2005 *IJBEM* **7** 62-5
[27] Le Van Quyen M, Adam C, Baulac M, Martinerie J and Varela F J 1998 *Brain Res.* **792** 24-40
[28] Lopes da Silva F H, Pijn J P and Wadman W J 1994 *Prog. Brain Res.* **102** 359-70
[29] Bullmore E T, Suckling J, Overmeyer S, Rabe-Hesketh S, Taylor E, Brammer M J **1999** *IEEE Transactions on Medical Imaging* 18 32-42